applied optics

Nonlinear refraction and absorption measurements of thin films by the dual-arm Z-scan method

Trenton R. Ensley,[1,2] Sepehr Benis,[1] Honghua Hu,[1] Zhong'an Li,[3,4] Sei-Hum Jang,[3] Alex K.-Y. Jen,[3,5] Joseph W. Perry,[6,7] Joel M. Hales,[6] David J. Hagan,[1] and Eric W. Van Stryland[1,*]

[1]CREOL: The College of Optics & Photonics, University of Central Florida, Orlando, Florida 32816, USA
[2]Current Address: U.S. Army Research Laboratory, Sensors and Electron Devices Directorate, Adelphi, Maryland 20783, USA
[3]Department of Materials Science and Engineering, University of Washington, Seattle, Washington 98195, USA
[4]Current Address: School of Chemistry and Chemical Engineering, Huazhong University of Science and Technology, 430074 Wuhan, China
[5]Current Address: Department of Chemistry, City University of Hong Kong, Kowloon, Hong Kong
[6]School of Chemistry & Biochemistry, Georgia Institute of Technology, Atlanta, Georgia 30332, USA
[7]Center for Organic Photonics & Electronics, Georgia Institute of Technology, Atlanta, Georgia 30332, USA
*Corresponding author: ewvs@creol.ucf.edu

Received 17 December 2018; revised 1 February 2019; accepted 15 February 2019; posted 19 February 2019 (Doc. ID 355371); published 18 March 2019

We extend the recently developed dual-arm Z-scan to increase the signal-to-noise ratio (SNR) for measuring the nonlinear refraction (NLR) of thin films on thick substrates. Similar to the case of solutes in solution, the phase shift due to NLR in a thin film can often be dominated by the phase shift due to NLR in the much thicker substrate. SNR enhancement is accomplished by simultaneously scanning a bare substrate and the film plus substrate in two separate but identical Z-scan arms. The subtraction of these signals taken simultaneously effectively cancels the nonlinear signal from the substrate, leaving only the signal from the film. More importantly, the SNR is increased since the correlated noise from effects such as beam-pointing instabilities cancels. To show the versatility of the dual-arm Z-scan method, we perform measurements on semiconductor and organic thin films, some less than 100 nm thick and with thicknesses up to 4 orders of magnitude less than the substrate.

https://doi.org/10.1364/AO.58.000D28

1. HISTORICAL INTRODUCTION

Nonlinear optics research at CREOL started at the time of its founding in 1987, when the group of Van Stryland, Soileau, and Hagan studied nonlinear refraction (NLR), nonlinear absorption (NLA), and optical damage [1], at that time mainly in inorganic materials. NLR and NLA are responsible for optical "self-action," where laser light of high irradiance can alter the refractive index, n, and absorption coefficient, α, of a material. The irradiance-dependent optical coefficients may be expressed in a power series as

$$n(I) = n_0 + n_2 I + n_4 I^2 + \ldots, \tag{1}$$

$$\alpha(I) = \alpha_0 + \alpha_2 I + \alpha_3 I^2 + \ldots, \tag{2}$$

where I is the irradiance, the "0" subscript corresponds to the linear coefficients, n_2 corresponds to the lowest order instantaneous, bound-electronic NLR, while n_4 and higher order terms are less commonly observed. The coefficients α_2 and α_3 correspond to 2- and 3-photon absorption, respectively. In this formulation it is assumed that all nonlinear responses are instantaneous so that index and absorption changes follow the time dependence of the irradiance exactly, which is not always the case. The lowest order terms are related to the third-order nonlinear susceptibility, $\chi^{(3)}$, as follows [2]:

$$n_2 = \frac{3}{4\varepsilon_0 n_0^2 c}\,\mathrm{Re}\{\chi^{(3)}\}, \tag{3}$$

$$\alpha_2 = \frac{3\omega}{2\varepsilon_0 n_0^2 c^2}\,\mathrm{Im}\{\chi^{(3)}\}, \tag{4}$$

where ε_0 is the vacuum permittivity, c is the speed of light, and ω is the optical frequency.

In those days, the primary method for measuring NLR was by measuring transmittance as the laser pulse energy was varied. This allowed Van Stryland *et al.* [3,4] to verify Wherrett's scaling rules for 2-photon absorption (2PA) in semiconductors that allow prediction of 2PA for any direct-gap semiconductor [5]. The NLR was often measured either by measuring the critical

power for self-focusing, or by observing beam distortion in the near and far fields [6,7]. These methods lacked sensitivity, requiring high irradiances for most measurements, and usually did not address the sign of the NLR, which in those days was thought to be always positive in transparent materials.

Studies were conducted regarding NLA and NLR and their various applications, which led to the study of excited-state absorbers that exhibit weak linear absorption that increases significantly with increasing irradiance, including metallo-organics [8] and semiconductors (free-carrier absorption) [9]. Both of these material systems offer the added advantage of exhibiting NLR due to the excited states that reduce the nonlinear transmission by distorting the shape of the input beam. In this case, the equations for NLR and NLA can be complicated, and the absorption and refraction coefficients are strongly dependent on excitation and relaxation dynamics and can be defined as follows:

$$\alpha(I,t) = \alpha_0 + \alpha_2 I + \sigma_{ex} N(I,t) + \ldots, \tag{5}$$

$$n(I,t) = n_0 + n_2 I + \sigma_r N(I,t) + \ldots, \tag{6}$$

$$\frac{dN}{dt} = \frac{\alpha_0 I(t)}{\hbar\omega} + \frac{\alpha_2 I^2(t)}{2\hbar\omega} - \frac{N}{\tau}, \tag{7}$$

where σ_{ex} is the excited-state cross section, $N(I,t)$ is the irradiance and time, t, dependent number density of the excited state, σ_r is the free-carrier cross section defined as the change in refractive index per unit photoexcited charge-carrier density N, τ is the relaxation time, and $\hbar$ is the reduced Planck's constant. Note that the excited-state population as expressed contains contributions only up to the third-order nonlinear response.

In 1989, in the recently founded CREOL nonlinear optics laboratories, a major advance in nonlinear optical characterization was made. By placing an aperture in the far field of nonlinear transmission measurements, Sheik-Bahae *et al.* [10] noticed that the aperture transmittance depended greatly on the exact positioning of the sample near focus. This was quickly recognized as being due to the nonlinear lensing in the sample. The authors proceeded to scan the sample, recording the transmittance as a function of the sample position Z with respect to focus; hence, they phrased the technique the Z-scan. The Z-scan was quickly recognized as an extremely simple and sensitive yet absolutely calibrated technique for characterizing nonlinear optical (NLO) materials [10,11]. In particular, the sign of the NLR is easily determined from the Z-scan, which proved it to be a more powerful method than the aforementioned techniques, while also allowing the simultaneous measurement of NLA and NLR.

One of the first interesting discoveries enabled by Z-scan was that the sign of the bound electronic n_2 changes from positive to negative in the region of 2PA, i.e., when $0.5E_g \le \hbar\omega < E_g$, where E_g is the energy bandgap. Noting the analogy with a linear absorption resonance contributing negatively to the linear refraction above resonance, Sheik-Bahae *et al.* [12,13] developed a method for connecting the dispersion of n_2 to the spectrum of 2PA via Kramers–Kronig (KK) relations [2]. This resulted in a remarkably simple analytical formula that gave the magnitude, bandgap scaling, and dispersion of NLR. The predictions of this simple formula have agreed with experimental data of most known semiconductors and dielectrics spanning more than 5 orders of magnitude [14]. This theory also predicted a fundamental limit to the all-optical-switching figure-of-merit developed by Mizrahi *et al.* [15] for semiconductors, which played an essential role in the progress of this field. More recently, extending the simple 2PA theory to nondegenerate 2PA, we have observed nearly 3 orders of magnitude 2PA enhancement along with enhancement of the associated NLR as prescribed by KK relations [2,11]. In measuring NLR in the presence of strong NLA, we also developed a new technique that has even better sensitivity to NLR than Z-scan and is a two-beam method that gives the temporal dependence of NLA and NLR: the beam-deflection technique [16]. We have used this method for measuring nonlinearities in semiconductors [17,18], organics [19–22], and gases; however, it is not simple to extract the nonlinearity of a solute in a solvent, or, as discussed in this paper, to separate the NLR of a thin film on a substrate.

The Z-scan technique also led to the rediscovery of the large cascaded second-order effects from frequency conversion that mimic themselves as NLA and NLR [23]. Studies of n_2 of KTP initially seemed to give inconsistent results and even sometimes showed a change in sign [24]. These effects were recognized as effective NLR due to "cascaded" second-order nonlinearities that can result in very large nonlinear phase shifts [25,26]. This led to the generation of many new results and consequent publications including the first demonstration of two-dimensional spatial solitons [27,28].

The Z-scan technique is, thus, regularly used for both NLR and NLA measurements. However, for the study of organics in solution, the study of NLA is typically much easier than NLR. When measuring the nonlinear properties of molecules in solution, the NLA of the solvent is usually small, and determination of α_2 for the solute is not problematic. However, this is not the case for NLR. Typically, the NLR per molecule of the solvent is much less than that of the solute, but the large density of solvent molecules yields a large net NLR that may dominate the signal due to the solute. Additionally, there is a contribution to the measured n_2 due to the cuvettes used to hold the samples. In cases where the n_2 of the solute is small, large discrepancies can arise when reporting the solute nonlinearity since the NLR of the solvent and cuvette must be subtracted from that of the solution. Thus, the determination of solute nonlinearities in regions where the NLR is similar to or much smaller than the solvent or cuvette has been difficult. The dual-arm (DA) Z-scan, in which the solvent and solution are scanned simultaneously, was introduced as a solution to this problem [29]. In this work, we expand upon this technique and demonstrate that it is also useful for extracting the NLR of a thin film on a relatively thick substrate.

Concluding our history of nonlinear materials characterization, we must explain that we at CREOL rely on collaborators from around the globe to prepare and send samples to us. It is thus appropriate that in this paper, we include authors who supplied us with samples for which data on the molecules studied have not previously been published (in thin-film or solution

form). Other materials have been published, except not in thin-film form, and those collaborators have chosen to be acknowledged [30–32].

2. CHARACTERIZATION OF NLR IN THIN FILMS

Optical materials, including engineered materials [33], need to have large nonlinearities to be suitable for applications, such as in all-optical-switching devices [34,35]. These devices require large optically induced phase shifts, such as those arising from n_2. To implement such materials into integrated devices, thin films have to be grown on relatively thick substrates, and the NLR and NLA of the material must be precisely measured. Although device applications are likely to employ guided propagation in the plane of the film, for measurement of the NLO properties it is more practical to propagate perpendicular to the plane of the film. The short propagation path involved in such a geometry for a thin film creates a challenge in measuring the relatively small phase shifts induced by NLR in the film as compared to that in the substrate. All substrates exhibit some NLR, and since the substrate is usually several orders of magnitude thicker, the nonlinear phase shift accumulated in the substrate can often dominate that effect in the film. This problem does not exist for NLA measurements, as it is usually possible to choose a substrate with no NLA in the spectral region of interest. This issue is very similar to extracting the contribution of the solute in a dilute solution where the effect of the NLR from solute can be dominated by the solvent, which was mitigated by the introduction of the aforementioned DA Z-scan. As alluded to in the previous section, the DA Z-scan simultaneously scans two samples on two identical Z-scan arms to discriminate their nonlinear signal difference. This method cancels the correlated noise induced by fluctuations of the excitation source (e.g., pulse energy, beam pointing instabilities, pulse-width changes, etc.), thereby increasing the signal-to-noise ratio (SNR) and enabling the measurement of n_2 and α_2 of the solute. It was shown that the SNR for n_2 could be enhanced by up to 1 order of magnitude to resolve solute signals. In this work, we apply a similar methodology to that described above to extract thin-film nonlinearities in the presence of large substrate signals.

3. EXPERIMENT

To perform Z-scans, the sample is scanned along the axis of a focused beam, and the transmittance is recorded as a function of the sample position T(Z) [11]. Placing a partially closed aperture (CA) in the far field allows for sensitivity to NLR (specifically n_2 in this work), whereas in the case of a fully open aperture (OA), the Z-scan is only sensitive to NLA (specifically α_2 in this work). Thus, the CA Z-scan is sensitive to both n_2 and α_2, whereas the OA Z-scan is sensitive to only α_2. When analyzing the CA Z-scan data, the α_2 value from the OA Z-scan may be used, allowing a one parameter fit to obtain n_2. In certain instances, typically when $2\pi n_2/(\lambda_0\alpha_2) > 1$, where λ_0 is the wavelength, the CA Z-scan normalized data can be divided by the normalized OA Z-scan data to obtain a signal devoid of NLA. We refer to this as CA/OA where the effect of NLA is essentially eliminated.

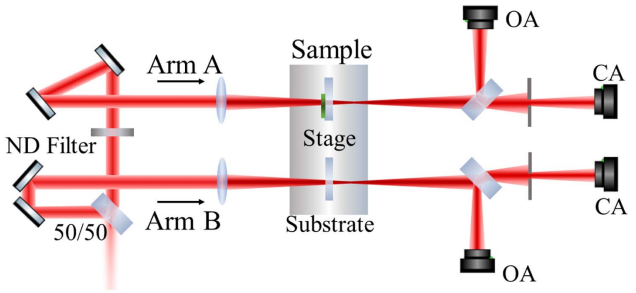

Fig. 1. Schematic of the DA Z-scan technique. The "ND filter" is a continuously variable neutral density filter to equalize the energy in each arm. "50/50" represents the beam splitter. "OA" and "CA" stand for open aperture and closed aperture, respectively.

Figure 1 shows the experimental configuration of the DA Z-scan technique to measure thin-film nonlinearities. To realize the enhancement in SNR, each arm of the DA Z-scan must be prepared to be as similar as possible by using matched optics. Furthermore, the irradiance distribution must be identical, i.e., pulse energy, beam waist, pulse width, and sample Z-position. The energy, beam waist, and pulse width equalization are described in detail in [29]. The sample and substrate are both mounted on a single stage and translated through the focus of the beams in two identical arms.

It is essential that the substrate used in each arm is identical. Thus, when preparing the films for deposition, substrates from the same lot are cleaved in two, yielding one blank reference and another on which the film is deposited [see Fig. 2(a)]. It is also essential to collocate the Z-positions of the two cleaved halves, and for this reason, the coated substrate must have a region that is left uncoated, which we label the "bare area." To collocate the Z-positions, the coated and uncoated substrates are each placed on 3-D stages on top of the main Z-scan stage. The coated substrate is translated until the bare area is in the beam path [see Fig. 2(a)]. This results in a signal showing only NLR from each arm (as there is no NLA from the substrate). The Z-positions are matched by adjusting the Z-position on one arm until the subtraction of the CA Z-scans yields a flat line [see Fig. 2(b)]. After this adjustment, the coated substrate is translated perpendicular to the beam so that the film is returned to the beam path [see Fig. 2(a)] for nonlinear characterization.

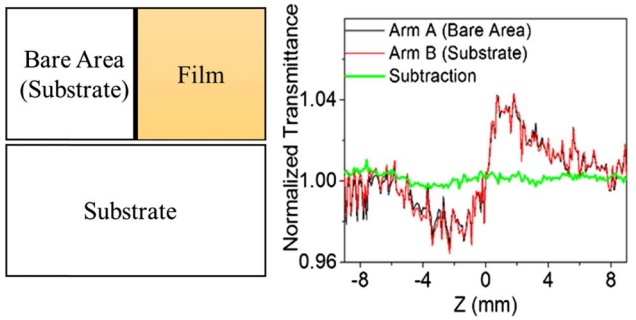

Fig. 2. (a) Method of film deposition such that the thickness is the same in each arm of the DA Z-scan. (b) Simultaneous CA Z-scans of Arm A and Arm B to match the Z-positions of the two samples.

4. RESULTS

To show the capability of the DA Z-scan in extracting the NLR and NLA of thin-film samples, we performed DA Z-scan measurements on both semiconductor and organic materials. A 3 μm thick ZnO film was fabricated on a 1 mm thick quartz substrate using radio frequency (RF) sputtering. The DA Z-scans were measured utilizing a Ti:sapphire regeneratively amplified system (Clark MXR, CPA 2110) at a wavelength of 780 nm with a pulsewidth of 170 fs (FWHM) at a 1 kHz repetition rate. It is important to note that when measuring thin films, large variations in the signal can arise due to sample inhomogeneity. To account for this, we perform low-energy background (LEB) subtraction as outlined in [29]. The LEB is a good qualitative measure of sample inhomogeneities. For the case of the ZnO thin films, the LEB subtraction along with a high-energy scan are shown in Fig. 3(a). Figure 3(b) shows the CA signal of the sample (film and substrate) and the substrate. Note that at a wavelength of 780 nm and peak irradiance, I_0, of 130 GW/cm^2, no nonlinear absorption signal is observed, which is expected at this wavelength. Figure 3 also shows a comparison of the ZnO thin films for the cases of (c) sequential Z-scans and (d) simultaneous DA Z-scans. The measured peak-to-valley change in transmittance, ΔT_{p-v}, from the 1 mm thick quartz substrate is 7× larger than that due to the ZnO film. The noise between the two sequential measurements is uncorrelated, yielding difficulties in extracting the thin-film NLR from sequential measurements. For the case of sequential Z-scans, i.e., Fig. 3(c), the signal of the ZnO film is buried within the noise. However, for the case of simultaneous subtraction, shown in Fig. 3(d), the signal is distinguishable above the noise. Other scans verified the NLR. The value of n_2 measured for the quartz substrate is $(2.1 \pm 0.5) \times 10^{-16}$ cm^2/W and agrees within reasonable error with previously reported literature values [36]. The value of $(1.0 \pm 0.6) \times 10^{-14}$ cm^2/W obtained from the ZnO thin film agrees within error with our measurements of bulk ZnO (thickness of 530 μm) of $(1.24 \pm 0.31) \times 10^{-14}$ cm^2/W using the same experimental configuration and is within a reasonable factor of the theoretical value of 2.4×10^{-14} cm^2/W [13] assuming $E_g = 3.3$ eV [37].

Figure 4 shows Z-scans of a 1.29 μm thick organic film of a highly polarizable anionic tricyanofuran cyanine, AJCPE04-TCF04, deposited on a 1 mm thick fused silica substrate. The neat films were deposited by spin-coating solutions on half of the substrate [as depicted in Fig. 2(a)]. Z-scan measurements were performed at 1300 nm generated by pumping an optical parametric amplifier (OPA, Light Conversion, Ltd. TOPAS-C) using 780 nm femtosecond pulses. There is no observed linear absorption from the film at this wavelength. In Figs. 4(a)–4(b), the OA and CA/OA signals are shown, respectively. The observed NLR is purely from the film after subtracting the effect of the quartz substrate and LEB in the DA Z-scan. Note that the quartz substrate does not have any NLA at this wavelength. In Fig. 4(c), the black curve shows the result for the case of a sequential Z-scan where measurements of the film plus substrate and the substrate were performed separately, and

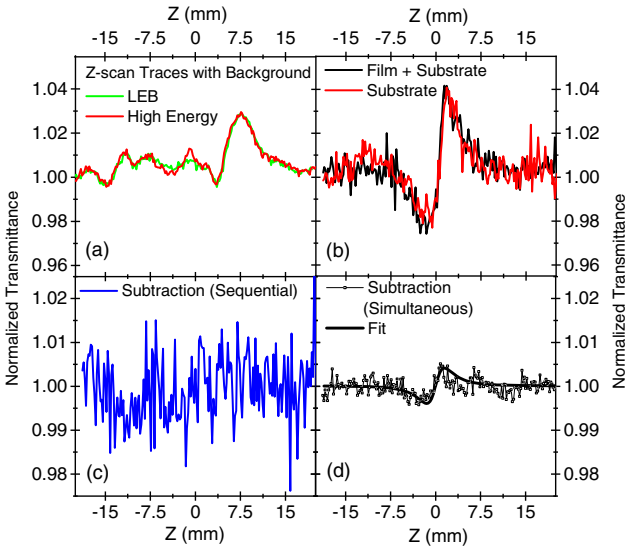

Fig. 3. (a) LEB along with high-energy scan of the ZnO thin film. (b) Z-scan measurements on film plus substrate and substrate. The two signals have uncorrelated noise. Comparison of the subtraction of the substrate CA Z-scan from the 3 μm ZnO film plus substrate CA Z-scan in the case of (c) sequential measurements and (d) simultaneous measurements (DA Z-scan) at a wavelength of 780 nm. The solid line in (d) is a fit.

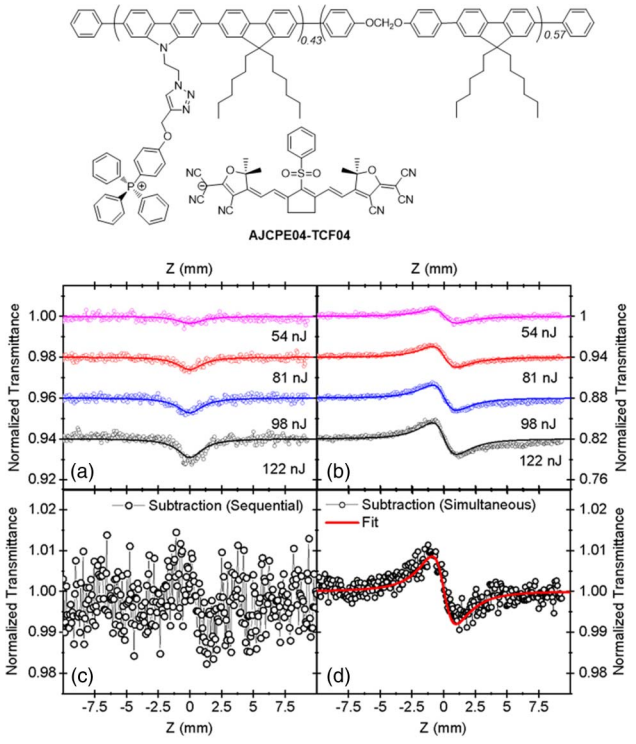

Fig. 4. DA Z-scan measurements of an organic film (AJCPE04-TCF04) of thickness 1.29 μm deposited on a 1 mm thick quartz substrate at a wavelength of 1300 nm using multiple irradiances, each offset for clarity. (a) and (b) are OA and CA/OA signals, respectively. The effects of substrate and LEB are subtracted from the signal. (c) Sequential measurements and (d) simultaneous measurements (DA Z-scan) show the comparison of the subtraction of the substrate CA/OA Z-scan from the film plus substrate CA/OA Z-scan in the case of 54 nJ input. The solid line in (d) is the best fit as in the top curve of (b).

the signal from the substrate was subtracted from that of the sample. In Fig. 4(d), the black curve shows the result of the DA Z-scan where measurements of the film plus substrate and substrate were performed simultaneously. This result shows ~5× enhancement in SNR when the DA Z-scan has been employed. The values of α_2 and n_2 measured for the film are 3.0 ± 0.6 cm/GW and $-(43 \pm 9) \times 10^{-14}$ cm^2/W, respectively. Note that the signal from the substrate is 2× larger than that due to the film.

An example of a measurement of a sub-100-nm thick film is shown in Figs. 5(a)–5(c). The sample is a polymethine chromophore doped in PMMA (7C-TCF-TOA:PMMA) film of thickness 90 nm deposited on a 1 mm thick BK7 substrate measured at a wavelength of 1550 nm, and a film of thickness 620 nm deposited on a similar substrate measured at a wavelength of 1400 nm [Fig. 5(d)]. This chromophore has been the subject of a previous study [30,31,38]. For these measurements, we use a different Ti:sapphire amplified system (Coherent, Legend Elite Duo HE+) producing 800 nm, 12 mJ, ~40 fs (FWHM) pulses at a 1 kHz repetition rate pumping an OPA (Light Conversion, Ltd. HE-TOPAS-Prime) to generate 1550 and 1400 nm pulses. Note that for these Z-scan measurements using pulse widths <50 fs (FWHM), a chirp compensation plate was placed in the reflected arm of Fig. 1, i.e., Arm B. The irradiance used for the data of Figs. 5(a) and 5(b) was 120 GW/cm^2 and for Fig. 5(d), 108 GW/cm^2. Note that at these irradiances, the ΔT_{p-v} from the BK7 substrate is around 2.2%. Thus, the signal from the film is small compared to that of the substrate. The CA/OA Z-scan in Fig. 5(a) was fit with an n_2 of $-(16 \pm 6) \times 10^{-13}$ cm^2/W. The OA Z-scan in Fig. 5(b) was fit with an α_2 of 23 ± 12 cm/GW, which is consistent with data from DA Z-scans taken at higher irradiances that also gave the same n_2 within errors. While α_2 agrees with the previously reported value of 22 cm/GW in Refs. [30,31], the n_2 reported herein is ~2.5× larger than the reported value of -5.9×10^{-13} cm^2/W. Figure 5(c) shows the LEB for this sample. The variation of the LEB over the scan is ~1.5%, while the ΔT_{p-v} is <1%. This indicates sample inhomogeneities in thickness and/or concentration that may account for some of the discrepancy. Another such discrepancy can arise due to ablation of the film surface when exposed to irradiances >100 GW/cm^2, as was observed in few-micrometer thick chalcogenide films in Ref. [39]. The ablation holes were observed to induce spurious NLR signals. To ensure this was not the case in our measurements, after Z-scan measurements at the largest irradiance, the LEB was rescanned to ensure that no changes in the Z-scan trace occurred.

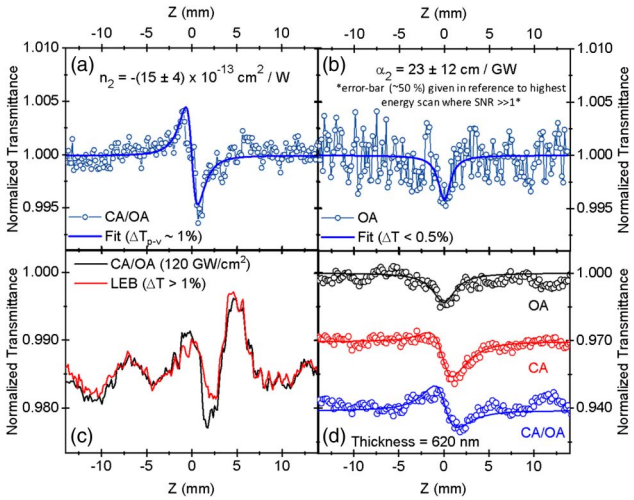

Fig. 5. (a) CA/OA and (b) OA DA Z-scan of the organic film of thickness 90 nm deposited on a 1 mm thick BK7 substrate measured at a wavelength of 1550 nm and peak irradiance of 120 GW/cm^2 after subtracting the effect of LEB. Solid lines are fits. (c) LEB and CA/OA signals at 120 GW/cm^2 before subtracting the LEB. (d) OA, CA, and CA/OA measurements on the organic film of thickness 620 nm deposited on a similar substrate at a measured wavelength of 1400 nm.

Figure 5(d) shows data for a thicker sample of the same material. We chose this particular sample, which was known by us to be of poor quality, with thickness variation indicated by the ~4% variation of the LEB as well as from independent thickness measurements, to illustrate that it is sometimes best to use CA Z-scan data without dividing by the OA Z-scan data. This division process can add unwanted noise as shown in the figure. The best way to analyze these data is to fit the OA data for the NLA and then use that value in fitting the CA Z-scan to obtain the NLR. This is possible for any type of Z-scan.

5. SUMMARY

In summary, we have extended the DA Z-scan technique to measure thin films on relatively thick substrates. By simultaneously measuring both film and substrate, the correlated noise in each arm is subtracted, allowing the determination of thin-film NLR signals up to 1 order of magnitude less than that of the substrate. Measurements of nonlinear refraction were performed on both semiconductor and organic thin films of thicknesses ranging from 90 nm to a few micrometers.

For a single component system, the DA Z-scan is not necessary as long as an identical reference arm is utilized, i.e., the reference arm takes the role of increasing the SNR [40]. It should not be expected that the sensitivity of the DA Z-scan to nonlinearly induced phase changes should be as good as when measuring a single component system. The primary advantage of the DA Z-scan is when the "background" NLR from a second material component obscures the NLR from the component of interest, in this case a thin film.

Funding. Army Research Laboratory (ARL) (W911NF-15-2-0090); National Science Foundation (NSF) (DMR-1609895); Air Force Office of Scientific Research (AFOSR) (FA9550-14-1-0040) MURI Center for Dynamic Magneto-Optics.

Acknowledgment. We greatly appreciate the following researchers who provided samples for characterization as well as many fruitful discussions of results: Alfred R. Ernst, Canek Fuentes-Hernandez, Amir Dindar, Bernard Kippelen, Seth R. Marder, and Jonathan D. Matichak, all from the Georgia Institute of Technology, Atlanta, GA, USA.

REFERENCES

1. M. Soileau, W. E. Williams, N. Mansour, and E. W. Van Stryland, "Laser-induced damage and the role of self-focusing," Opt. Eng. **28**, 281133 (1989).

2. D. C. Hutchings, M. Sheik-Bahae, D. J. Hagan, and E. W. Van Stryland, "Kramers-Krönig relations in nonlinear optics," Opt. Quantum Electron. **24**, 1–30 (1992).
3. E. W. Van Stryland, S. Guha, H. Vanherzeele, M. Woodall, M. Soileau, and B. Wherrett, "Verification of the scaling rule for two-photon absorption in semiconductors," Opt. Acta **33**, 381–386 (1986).
4. E. W. Van Stryland, M. Woodall, H. Vanherzeele, and M. Soileau, "Energy band-gap dependence of two-photon absorption," Opt. Lett. **10**, 490–492 (1985).
5. B. Wherrett, "Scaling rules for multiphoton interband absorption in semiconductors," J. Opt. Soc. Am. B **1**, 67–72 (1984).
6. S. Guha, E. W. Van Stryland, and M. Soileau, "Self-defocusing in CdSe induced by charge carriers created by two-photon absorption," Opt. Lett. **10**, 285–287 (1985).
7. M. Soileau, S. Guha, W. E. Williams, E. W. Van Stryland, H. Vanherzeele, J. Pohlmann, E. Sharp, and G. Wood, "Studies of the nonlinear switching properties of liquid crystals with picosecond pulses," Mol. Cryst. Liq. Cryst. **127**, 321–330 (1985).
8. T. Wei, D. Hagan, M. Sence, E. Van Stryland, J. Perry, and D. Coulter, "Direct measurements of nonlinear absorption and refraction in solutions of phthalocyanines," Appl. Phys. B **54**, 46–51 (1992).
9. A. Said, M. Sheik-Bahae, D. J. Hagan, T. Wei, J. Wang, J. Young, and E. W. Van Stryland, "Determination of bound-electronic and free-carrier nonlinearities in ZnSe, GaAs, CdTe, and ZnTe," J. Opt. Soc. Am. B **9**, 405–414 (1992).
10. M. Sheik-Bahae, A. A. Said, and E. W. Van Stryland, "High-sensitivity, single-beam n_2 measurements," Opt. Lett. **14**, 955–957 (1989).
11. M. Sheik-Bahae, A. A. Said, T.-H. Wei, D. J. Hagan, and E. W. Van Stryland, "Sensitive measurement of optical nonlinearities using a single beam," IEEE J. Quantum Electron. **26**, 760–769 (1990).
12. M. Sheik-Bahae, D. J. Hagan, and E. W. Van Stryland, "Dispersion and band-gap scaling of the electronic Kerr effect in solids associated with two-photon absorption," Phys. Rev. Lett. **65**, 96–99 (1990).
13. M. Sheik-Bahae, D. C. Hutchings, D. J. Hagan, and E. W. Van Stryland, "Dispersion of bound electron nonlinear refraction in solids," IEEE J. Quantum Electron. **27**, 1296–1309 (1991).
14. R. DeSalvo, A. A. Said, D. J. Hagan, E. W. Van Stryland, and M. Sheik-Bahae, "Infrared to ultraviolet measurements of two-photon absorption and n_2 in wide bandgap solids," IEEE J. Quantum Electron. **32**, 1324–1333 (1996).
15. V. Mizrahi, K. DeLong, G. I. Stegeman, M. A. Saifi, and M. Andrejco, "Two-photon absorption as a limitation to all-optical switching," Opt. Lett. **14**, 1140–1142 (1989).
16. M. R. Ferdinandus, H. Hu, M. Reichert, D. J. Hagan, and E. W. Van Stryland, "Beam deflection measurement of time and polarization resolved ultrafast nonlinear refraction," Opt. Lett. **38**, 3518–3521 (2013).
17. S. Benis, D. J. Hagan, and E. W. Van Stryland, "Enhancement mechanism of nonlinear optical response of transparent conductive oxides at epsilon-near-zero," in *CLEO: QELS Fundamental Science* (Optical Society of America, 2018), paper FF2E. 1.
18. P. Zhao, M. Reichert, D. J. Hagan, and E. W. Van Stryland, "Dispersion of nondegenerate nonlinear refraction in semiconductors," Opt. Express **24**, 24907–24920 (2016).
19. S. Benis, D. J. Hagan, and E. W. Van Stryland, "Cross-propagating beam-deflection measurements of third-order nonlinear optical susceptibility," Proc. SPIE **10088**, 100880N (2017).
20. M. Reichert, H. Hu, M. R. Ferdinandus, M. Seidel, P. Zhao, T. R. Ensley, D. Peceli, J. M. Reed, D. A. Fishman, and S. Webster, "Temporal, spectral, and polarization dependence of the nonlinear optical response of carbon disulfide," Optica **1**, 436–445 (2014).
21. M. Reichert, H. Hu, M. R. Ferdinandus, M. Seidel, P. Zhao, T. R. Ensley, D. Peceli, J. M. Reed, D. A. Fishman, and S. Webster, "Temporal, spectral, and polarization dependence of the nonlinear optical response of carbon disulfide: erratum," Optica **3**, 657–658 (2016).
22. P. Zhao, M. Reichert, S. Benis, D. J. Hagan, and E. W. Van Stryland, "Temporal and polarization dependence of the nonlinear optical response of solvents," Optica **5**, 583–594 (2018).
23. N. Belashenkov, S. Gagarskii, and M. Inochkin, "Nonlinear refraction of light on second-harmonic generation," Opt. Spectrosc. **66**, 806–808 (1989).
24. R. DeSalvo, D. J. Hagan, M. Sheik-Bahae, G. Stegeman, E. W. Van Stryland, and H. Vanherzeele, "Self-focusing and self-defocusing by cascaded second-order effects in KTP," Opt. Lett. **17**, 28–30 (1992).
25. G. Assanto, Z. Wang, D. Hagan, and E. Van Stryland, "All-optical modulation via nonlinear cascading in type II second-harmonic generation," Appl. Phys. Lett. **67**, 2120–2122 (1995).
26. Z. Wang, D. J. Hagan, E. W. Van Stryland, J. Zyss, P. Vidakovik, and W. E. Torruellas, "Cascaded second-order effects in N-(4-nitrophenyl)-L-prolinol, in a molecular single crystal," J. Opt. Soc. Am. B **14**, 76–86 (1997).
27. W. E. Torruellas, Z. Wang, D. J. Hagan, E. W. VanStryland, G. I. Stegeman, L. Torner, and C. R. Menyuk, "Observation of two-dimensional spatial solitary waves in a quadratic medium," Phys. Rev. Lett. **74**, 5036–5039 (1995).
28. B. Zhou, A. Chong, F. Wise, and M. Bache, "Ultrafast and octave-spanning optical nonlinearities from strongly phase-mismatched quadratic interactions," Phys. Rev. Lett. **109**, 043902 (2012).
29. M. R. Ferdinandus, M. Reichert, T. R. Ensley, H. Hu, D. A. Fishman, S. Webster, D. J. Hagan, and E. W. Van Stryland, "Dual-arm Z-scan technique to extract dilute solute nonlinearities from solution measurements," Opt. Mater. Express **2**, 1776–1790 (2012).
30. S. Jakobs, A. Petrov, J. W. Perry, J. M. Hales, S. Marder, and M. Eich, "Four wave mixing in silicon-organic hybrid waveguides," in *Advanced Photonics Congress*, OSA Technical Digest (online) (Optical Society of America, 2012), paper NTh1A.1.
31. J. M. Hales, H. Kim, A. DeSimone, H. Wen, T. Hou, A. K. Y. Jen, S. R. Marder, M. Lipson, A. L. Gaeta, and J. W. Perry, "Materials for loss-based switching in silicon-organic hybrid devices," in *Advanced Photonics Congress*, OSA Technical Digest (online) (Optical Society of America, 2012), paper NTh1A.2.
32. T. R. Ensley, H. Hu, A. R. Ernst, C. Fuentes-Hernandez, A. Dindar, B. Kippelen, D. J. Hagan, and E. W. Van Stryland, "Nonlinear refraction measurements of thin films by the dual-arm Z-scan method," in *Nonlinear Optics 2013*, OSA Technical Digest (online) (Optical Society of America, 2013), paper NTu1B.4.
33. V. P. Drachev, A. V. Kildishev, J. D. Borneman, K.-P. Chen, V. M. Shalaev, K. Yamnitskiy, R. A. Norwood, N. Peyghambarian, S. R. Marder, and L. A. Padilha, "Engineered nonlinear materials using gold nanoantenna array," Sci. Rep. **8**, 780 (2018).
34. J. M. Hales, J. Matichak, S. Barlow, S. Ohira, K. Yesudas, J.-L. Brédas, J. W. Perry, and S. R. Marder, "Design of polymethine dyes with large third-order optical nonlinearities and loss figures of merit," Science **327**, 1485–1488 (2010).
35. G. I. Stegeman and R. H. Stolen, "Waveguides and fibers for nonlinear optics," J. Opt. Soc. Am. B **6**, 652–662 (1989).
36. D. Milam, "Review and assessment of measured values of the nonlinear refractive-index coefficient of fused silica," Appl. Opt. **37**, 546–550 (1998).
37. V. Srikant and D. R. Clarke, "On the optical band gap of zinc oxide," J. Appl. Phys. **83**, 5447–5451 (1998).
38. Z. A. Li, Y. Liu, H. Kim, J. M. Hales, S. H. Jang, J. Luo, T. Baehr-Jones, M. Hochberg, S. R. Marder, and J. W. Perry, "High-optical-quality blends of anionic polymethine salts and polycarbonate with enhanced third-order non-linearities for silicon-organic hybrid devices," Adv. Mater. **24**, OP326–OP330 (2012).
39. K. Fedus, G. Boudebs, C. B. D. Araújo, M. Cathelinaud, F. Charpentier, and V. Nazabal, "Photoinduced effects in thin films of $Te_{20}As_{30}Se_{50}$ glass with nonlinear characterization," Appl. Phys. Lett. **94**, 061122 (2009).
40. H. Ma, A. S. L. Gomes, and C. B. de Araujo, "Measurements of nondegenerate optical nonlinearity using a two-color single beam method," Appl. Phys. Lett. **59**, 2666–2668 (1991).